Original Article

Relationship between peripapillary vessel density and visual function based on Garway-Heath sectorization in open-angle glaucoma

Jeong Min Kwon[1], Keunheung Park[2,3], Sangyoon Kim[4], Jonghoon Shin[4,5]

Purpose: To investigate the relationship between peripapillary vessel density (pVD) and visual field sensitivity (VFS) and between peripapillary retinal nerve fiber layer thickness (pRNFLT) and VFS, based on Garway-Heath sectorization in open-angle glaucoma patients. **Methods:** Sixty-six eyes of healthy subjects and 84 eyes of glaucoma subjects were included. All subjects underwent several eye examinations, including standard automated perimetry and optical coherence tomography angiography. Sectoral structure-function relationships based on the Garway-Heath sectorization were compared among normal subjects, the 'mild glaucoma,' and 'moderate-to-severe glaucoma' group. Multivariate analyses were performed for each sector to determine the factors related to VFS. The diagnostic abilities of vessel density parameters and RNFLT were evaluated by calculating the area under the receiver operating characteristic curves (AUROC). **Results:** The correlation between pVD-VFS and pRNFLT-VFS was statistically significant in the glaucoma group independent of the VFS sector. In the glaucoma group, VFS in the temporal sector was statistically related in a multivariate model to pVD, pRNFLT and age ($R^2 = 0.721$; $P = 0.007$, < 0.001, .15, respectively). We found pRNFLT and age were significantly associated with VFS in glaucoma. The AUROC values of pVD in the inferotemporal sector of the total, mild, and moderate-to-severe glaucoma (0.843, 0.714, and 0.972, respectively) were comparable to pRNFLT in this sector (0.833, 0.718, 0.948, respectively). **Conclusion:** Since the relationship between pVD and VFS in the papillomacular area was significant, measuring pVD and RNFLT in the corresponding area will be valuable in expanding our pathophysiologic knowledge of the paracentral field defects in glaucoma.

Access this article online

Website: www.ijo.in

DOI: 10.4103/ijo.IJO_2904_20

Quick Response Code:

Key words: Glaucoma, optical coherence tomography angiography, papillomacular area, peripapillary vessel density

Glaucoma is a progressive optic neuropathy that causes specific damage to optic nerve fibers resulting in visual field defects (VFDs).[1] Intraocular pressure (IOP), related mechanical, stress and vascular insufficiency of the optic nerve are the principal causes underlying the anatomical and functional damage in glaucoma. However, the exact mechanisms are unknown.[2,3] The visual field (VF) loss in normal-tension glaucoma (NTG) is more localized and manageable compared to high tension glaucoma.[4] Also, glaucoma patients with central field defects have higher systemic risk factors such as hypotension, migraine, Raynaud's phenomenon, and sleep apnea than those with nasal step defects.[5] Since the retinal ganglion cell axons in the papillomacular bundle region correlate with central visual function, we speculated that an eye with a more vulnerable optic nerve vasculature might have VFDs in the more central area, including the papillomacular bundle region corresponding to the paracentral field.

The development of optical coherence tomography angiography (OCT-A) has enabled noninvasive measurements of vascular changes in the peripapillary or parafoveal area, and OCT-A has been increasingly used in retinal diseases and glaucoma.[6-8] Previous studies have revealed a significant association between abnormal vessel density (VD) in the peripapillary area and glaucomatous optic neuropathy.[9-11] Despite the importance of preserving the central field in glaucoma, the structural OCT image might have some limitations in obtaining these areas' information.[12,13] In analyzing the relationship between VD and function in the papillomacular bundle region, the sectoral relationship between VD and visual field sensitivity (VFS) in glaucoma has not been discussed.

The present study had two primary purposes: 1) to sectorally compare the correlation between peripapillary vessel density (pVD) and VFS with that between peripapillary retinal nerve fiber layer thickness (pRNFLT) and VFS, and 2)

[1]Department of Ophthalmology, Pusan Veterans Hospital, Busan, South Korea, [2]Department of Ophthalmology, Pusan National University College of Medicine, Busan, Korea, [3]Department of Ophthalmology, Pusan Medical Center, Busan, Korea, [4]Department of Ophthalmology, Pusan National University School of Medicine, Yangsan, South Korea, [5]Department of Ophthalmology, Research Institute for Convergence of Biomedical Science and Technology, Pusan National University Yangsan Hospital, Yangsan, South Korea

Corresponding to: Dr. Jonghoon Shin, Department of Ophthalmology, Pusan National University School of Medicine, 20 Geumo-ro, Mulgeum-eup, Yangsan-si, Gyeongsangnam-do, South Korea. E-mail: jjongggal@naver.com

Received: 12-Sep-2020 Revision: 26-Jan-2021
Accepted: 08-Feb-2021 Published: 18-Jun-2021

Cite this article as: Kwon JM, Park K, Kim S, Shin J. Relationship between peripapillary vessel density and visual function based on Garway-Heath sectorization in open-angle glaucoma. Indian J Ophthalmol 2021;69:1825-32.

to evaluate the VFS determinants in each sector, including papillomacular bundle region. The secondary objective was to perform sectoral comparisons of the diagnostic abilities of pVD and pRNFLT based on the glaucoma severity.

Methods

Subjects: This was a prospective, cross-sectional, and comparative study in a single institute. The institutional review board of our institution approved this study, and all procedures were executed following the principles of the Declaration of Helsinki. We recruited patients with glaucoma (glaucoma group) and healthy subjects without glaucoma (control group) from our institution's glaucoma clinic. Each patient was informed of the purpose and procedures of this study and provided written consent to participate. This study was registered as an interventional study in the ISRCTN registry. When both eyes were eligible, one eye was randomly selected for inclusion in the study.

All study participants underwent a complete ophthalmic examination, including measurement of best-corrected visual acuity (BCVA), slit-lamp examination, IOP measurement with Goldmann tonometry, gonioscopy, funduscopy, and standard automated perimetry. Central corneal thickness (CCT) was measured using ultrasonic pachymetry (Pachmate; DGH Technology, Exton, PA). Keratometry was performed with an auto kerato-refractometer (RK-F2; CANON, Kanagawa, Japan). Red-free RNFL photographs and optic disc photographs were also examined. OCT examinations were performed to measure pVD and pRNFLT.

For inclusion in the study, all subjects in the glaucoma group had to have a clinical diagnosis of glaucoma regardless of their current IOP levels. The inclusion criteria were: BCVA better than or equal to 20/40, spherical equivalent between −6.00 and +3.00 diopters (D) and cylinder correction within ±3.00 D, no media opacities, a normal anterior chamber on slit-lamp examination, and open-angles on gonioscopy. Exclusion criteria included non-glaucomatous neuropathies, retinal diseases, and prior intraocular surgery, except cataract surgery. Glaucoma was defined as asymmetric inter-eye cup-to-disc ratio ≥0.2, vertical cup-to-disc ratio >0.7, neural rim thinning, localized notching, disc hemorrhage, and RNFL defects with corresponding glaucomatous VFDs.[1] An automated VF examination was performed with a standard 24-2 SITA program on a Humphrey 740 Visual Field Analyzer (HFA 740; Carl Zeiss Meditec, Dublin, CA). We defined glaucomatous VF based on the presence of two of the three following criteria: (1) an abnormal glaucoma hemifield test (a borderline score was not considered abnormal), (2) three continuous non-edge points (allowing for two-step nasal edge points) with $P < 0.05$ for the total deviation plot and $P < 0.01$ for at least one point, and (3) $P < .05$ for pattern standard deviation (PSD) on the SITA Standard test. Reliable VF tests had a false-positive rate < 15%, false-negative rate < 15%, and fixation loss < 20%. The severity of glaucomatous damage was classified as mild (VF mean deviation (MD) ≥ −6 dB) or moderate-to-severe (VF MD < −6 dB).[1] The subjects' eyes in the normal control group had an IOP < 21 mmHg, no glaucomatous optic disc changes, a normal VF, and no ocular disease history.

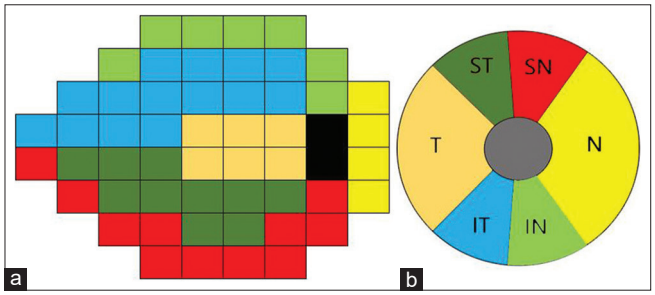

Figure 1: Division of the visual field (a) and optic nerve head (b) into sectors of a right eye based on the Garway-Heath map. We set temporal (t), inferotemporal (IT), superotemporal (ST), inferonasal (IN), superonasal (SN), and nasal (N) sectors to sectors 1, 2, 3, 4, 5, and 6, respectively

OCT-A imaging and pVD measurements: We used a swept source-OCT (SS-OCT, DRI OCT-1 Atlantis; Topcon, Tokyo, Japan) that uses infrared light with a wavelength of 1050 nm, at a rate of 100,000 axial scans (A-scans) per second to obtain OCT-A images. The infrared light signal has a wavelength longer than the conventional spectral domain-OCT, thus enabling deeper penetration of the retina and choroid. Its axial and transverse resolutions are 7 and 20 μm in tissue, respectively. Volumetric OCT scans were acquired from 6 × 6 mm cubes. Each cube consisted of 320 clusters of four repeated two-dimensional transverse scans (B scans) centered on the disc.

Two investigators reviewed all the scans for signal strength, segmentation error, loss of fixation, and motion artifact as part of the quality assessment. Eyes with poor image quality were excluded based on the following criteria: (1) poor fixation resulting in a double vessel pattern and motion artifacts, (2) media opacity obscuring the vessel signal in the field of view, or a signal strength index less than 7, and (3) segmentation error resulting in poor outlining of vascular networks. We detected blood flow by measuring intensity fluctuations from the scanned OCT images. In this technique known as OCT-A ratio analysis (OCTARA), calculations are based on the intensity values' ratio across points within one scan and identical points in repeated scans. OCTARA provides a relative sensitivity advantage of the magnitude of ten to 50 times for medium to low blood flow.

We performed automated segmentation using OCT software to separate each layer of the retina. The peripapillary sector was defined as a 0.75 mm-wide elliptical annulus extending from the inner elliptical contour (optic disc boundary). To measure the pVD, we used the average and sectoral pVD values in the radial peripapillary capillary layer, which extends from the inner limiting membrane to the outer limit of the RNFL.[14] The software automatically fit an ellipse to the disc margin based on the OCT en-face image. The software provided six peripapillary sectors based on the Garway-Heath map[15]: temporal (T, 311° to 40°), superotemporal (ST, 41° to 80°), superonasal (SN, 81° to 120°), nasal (N, 121° to 230°), inferonasal (IN, 231° to 270°) and inferotemporal (IT, 271° to 310°).

We developed custom software using Microsoft Visual Studio 2012 and the C# language with a dot net library that calculates the average sectoral VD according to the Garway-Heath map sectors [Fig. 1]. This software required superficial vascular layer image data and a color VD map exported from the OCT-A instrument. The optic disc was detected automatically after

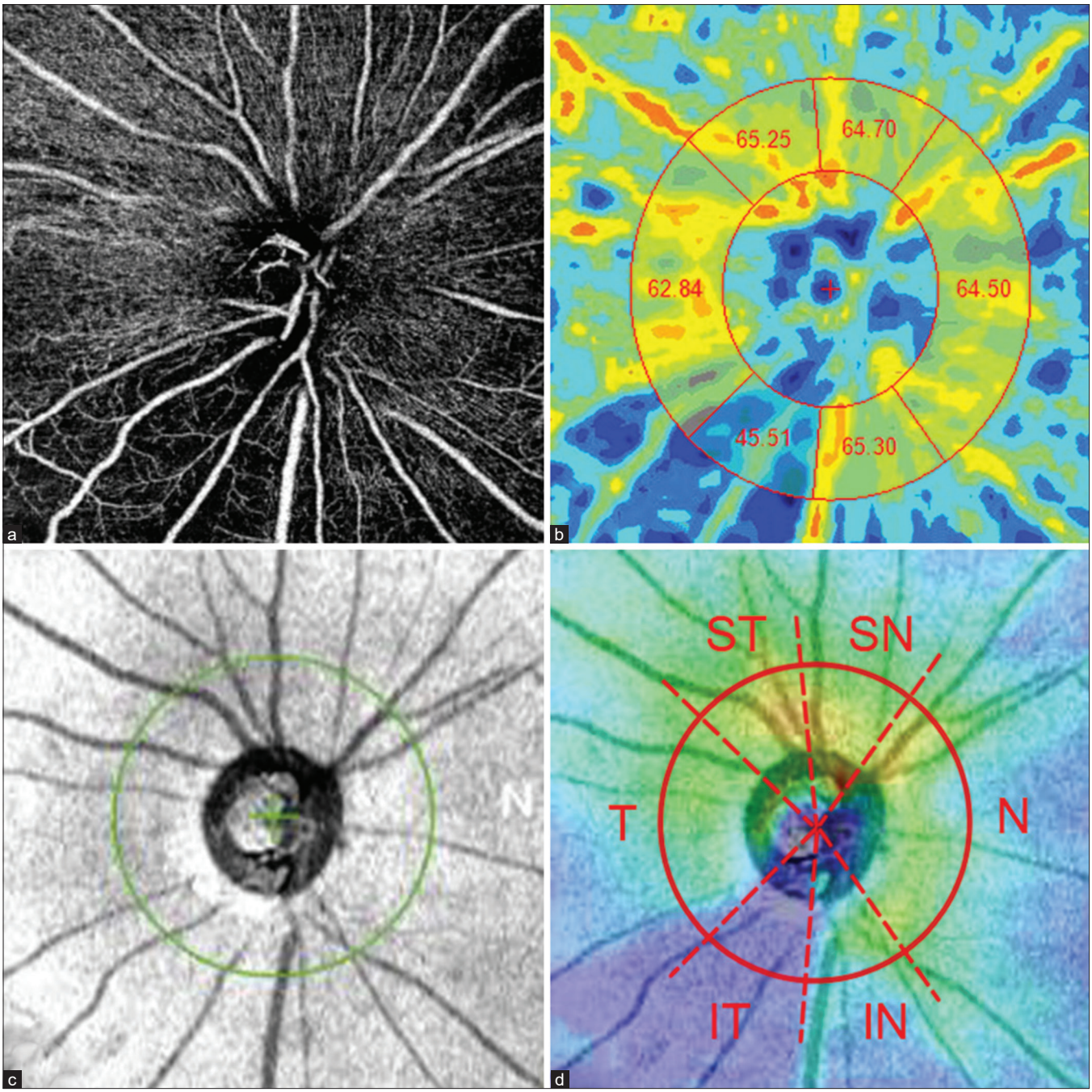

Figure 2: Representative case of a right eye showing localized attenuation of the vessel density in the inferotemporal (IT) area and decreased peripapillary retinal nerve fiber layer (pRNFL) thickness in the IT area. (a) Optical coherence tomography angiography (OCT-A) en-face image of the radial peripapillary capillary layer; (b) A color vessel density map, exported from OCT-A showing the peripapillary vessel density of the six sectors corresponding to the Garway-Heath map; (c, d) An infrared image and pRNFL thickness map of the optical coherence tomography

these two image files have been loaded. The user also had the option to manually set the optic disc location if the software failed to do so. The software then calculated the mean sectoral VD of the two ellipsoidal boundaries.

RNFLT measurements: We performed wide-angle scanning with SS-OCT to obtain circumpapillary RNFLT measurements. The wide-angle scanning uses a wide-angle 12 × 9 mm lens. SS-OCT automatically detects the disc's center, after which it draws a peripapillary circle (3.46 mm diameter). The method for measuring RNFLT using the OCT protocol for glaucoma has been described elsewhere.[3,4] We analyzed the average RNFLT and six sectoral RNFLTs (T, ST, SN, N, IN, and IT) matching the pVD sectors. A representative case of the peripapillary scan is presented in the Fig. 2.

Sectoral Relationship between the structure (pVD and RNFLT) and VF defect: The mean VFS in various sectors was defined as the average value of the differential light sensitivity (DLS) obtained at VF test locations corresponding

to pVD sectors. The VFS was expressed in unlogged 1/L scales (L, luminance measured in lamberts). The DLS at each tested location can be simply expressed as DLS = 10 × log10 (1/L) in decibels. The non-logarithmic 1/L value at each tested location was calculated by dividing the decibel reading by ten prior to deriving the antilogarithm. Using the segmentation by Garway-Heath *et al*.,[15] regional relationships between the VFS and each pVD or RNFLT were assessed, respectively. The HFA 24-2 test points were also grouped into six sectors.

Statistical analysis: We used the one-way analysis of variance (ANOVA) test to compare demographic and clinical data, OCT-A VD, and RNFLT among normal, mild, and moderate-to-severe glaucoma groups, and if the *P* value in the ANOVA test were less than 0.05, post hoc analysis (Tukey's test) was performed. Categorical variables were compared using the Chi-square test. A Spearman's correlation test was used to investigate the correlation of pVD-VFS and pRNFLT-VFS in each sector. In all regression tests assessing vasculature-function and structure-function relationships, pVD and pRNFLT were treated as the independent variables and the corresponding VFS as the dependent variable. When expressed in a linear unlogged 1/L scale, the VFS showed the structure-function relationship better, so we used linear regression analysis to evaluate the relationship between pVD or pRNFLT and VFS. We further compared correlation coefficients of pVD-VFS and pRNFLT-VFS of normal, mild, and moderate-to-severe glaucoma groups in each sector. We computed Pearson's correlation coefficient and used Fisher's z test to assess the significance of the correlation. We used the single and multiple linear regression analysis to evaluate if factors such as age, gender, spherical equivalent, CCT, hypertension, diabetes mellitus, pVD, and RNFLT were associated with VFS. The diagnostic abilities of the vessel density parameters and RNFLT for differentiating the normal control group and mild, moderate-to-severe, and total (mild and moderate-to-severe) glaucoma groups were evaluated by calculating the area under the receiver operating characteristic curves (AUROC). We used the SPSS version 20.0 (SPSS, Chicago, IL) to perform all statistical analyses, with statistical significance set at $P \leq 0.05$.

Results

We studied a total of 66 eyes from healthy control subjects and 84 eyes from glaucoma subjects. Table 1 shows the demographic and clinical characteristics in normal contr ol and glaucoma groups. We found statistically significant differences between normal control and glaucoma groups in VF mean deviation (MD), VF PSD, pVD, and RNFLT ($P < 0.001$). Other demographic and ocular factors, such as age, sex, laterality, IOP, SE, CCT, and history of hypertension and diabetes, were comparable between the groups.

We compared correlation in total, mild, and moderate-to-severe glaucoma with those of normal controls [Fig. 3]. Sectoral correlation coefficients of pVD-VFS and pRNFLT-VFS were significantly higher in total glaucoma than in normal subjects, except for pVD-VFS in sector 5 ($P < 0.001$, < 0.001 in sector 1; < .001, < .001 in sector 2; < .001, < .001 in sector 3; < .001, 0.018 in sector 4; 0.190, 0.042 in sector 5; 0.045, < .001 in sector 6). The correlation coefficient of pVD-VFS in sectors 1, 2 and 4, and pRNFLT-VFS in sector 2 were significantly higher in mild glaucoma than in normal control subjects ($P = .041, .003, .036, .036$, respectively). The correlation coefficient of pVD-VFS in sectors 1, 2, and 3, and pRNFLT-VFS in sectors 3 and 6 were significantly higher in moderate-to-severe glaucoma than in normal control subjects. ($P = .004, .004, .008, .022, .011$, respectively).

A multivariate regression analysis [Table 2] showed that pVD, pRNFLT and age were significantly independent parameters on VFS in glaucoma, in sector 1 ($R^2 = 0.721$; $P = 0.007$, < 0.001, 0.015, respectively). In the other sectors, pRNFLT and age were significantly associated with VFS in glaucoma ($R^2 = 0.808$, $P < 0.001$; $R^2 = 0.764$, $P < .001$; $R^2 = 0.706$, $P < .001$; $R^2 = 0.614$, $P < .05$; $R^2 = 0.601$, $P < .05$, respectively in sectors 2 to 6).

The diagnostic ability of zonal pRNFLT and pVD to detect different stages of glaucoma are shown in Table 3. In sector 2, pRNFLT and pVD had the highest AUROC values of 0.718 and 0.714 respectively in early glaucoma, 0.948 and 0.972 respectively in moderate-to-severe glaucoma, and 0.833 and 0.843 respectively in total glaucoma. Also, in sector 2, the AUROC values of pVD of total, mild and moderate-to-severe glaucoma were comparable to those of pRNFLT ($P = 0.759$, 0.945, .163, respectively).

Discussion

The present study has shown that a statistically significant sectoral relationship exists between pVD and VFS and between pRNFLT and VFS in glaucoma regardless of VFS location. In the glaucoma group, the pVD is significantly correlated with VFS only on the temporal peripapillary sectors that represent most of the papillomacular area, and the pRNFLT and age are significantly associated with VFS in all sectors.

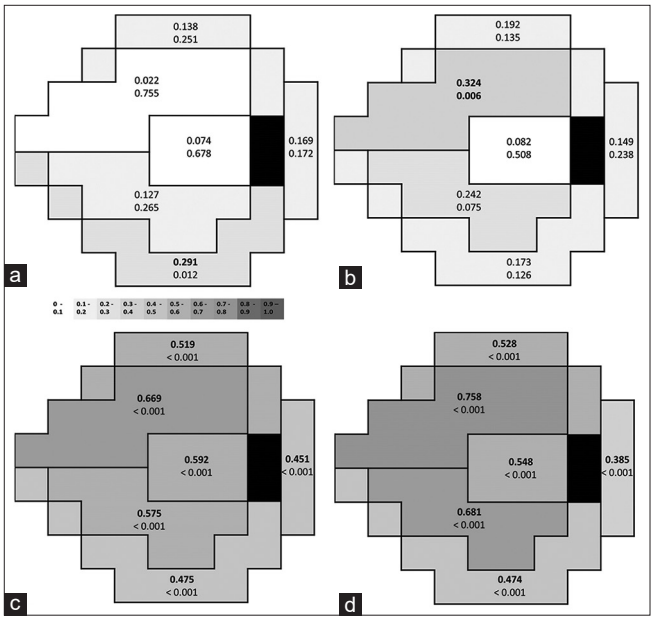

Figure 3: The correlation between visual field sensitivity and peripapillary vessel density (pVD) and peripapillary retinal nerve fiber layer thickness (pRNFLT) of each sector based on the Garway-Heath map in normal subjects (a and b) and total glaucoma (c and d). The gray-scale correlation coefficients (r_s) ranges are shown at the bottom; darker gray color means higher r_s in the scatter plot. The upper-case characters show r_s, and lower-case characters show *P* values of r_s. An old letter means significant r_s in the sector

Table 1: Demographics and clinical characteristics in the normal control and glaucoma groups.

	Control group	Glaucoma group		*P*‡	*P*§	*P*‖	*P*¶
	Normal (*n*=66)	Mild (*n*=42)	Moderate-to-severe (*n*=42)				
Age (years)*	54.4±15.0	57.7±13.1	61.2±13.7	0.053			
Sex (male/female)†	32/34	22/20	24/18	0.679			
Laterality (right/left)†	42/24	18/24	22/20	0.101			
Intraocular pressure (mmHg)*	14.2±3.7	13.9±2.4	15.5±5.7	0.170			
Spherical equivalent (D) *	-0.4±2.2	-0.7±2.0	-1.2±2.6	0.213			
CCT (㎛) *	543.7±33.1	555.7±31.7	546.9±43.6	0.324			
History of hypertension (*n*, %) [b]	10 (15.1)	11 (26.2)	15 (35.7)	0.047			
History of diabetes (*n*, %)†	10 (15.1)	7 (16.7)	7 (16.7)	0.969			
Visual field, MD (dB) *	0.2±1.0	-1.4±2.4	-13.9±6.0	<0.001	0.047	<0.001	<0.001
Visual field, PSD (dB) *	2.2±0.8	3.6±2.5	12.5±3.1	<0.001	0.002	<0.001	<0.001
pVD (%)*							
Sector 1 (T)	63.9±1.4	62.7±2.9	59.6±3.3	<0.001	0.038	<0.001	<0.001
Sector 2 (IT)	64.0±1.5	61.6±4.5	55.3±5.0	<0.001	0.004	<0.001	<0.001
Sector 3 (ST)	63.3±1.8	62.5±1.9	59.0±4.4	<0.001	0.427	<0.001	<0.001
Sector 4 (IN)	62.7±2.3	61.3±3.9	58.3±4.5	<0.001	0.158	<0.001	<0.001
Sector 5 (SN)	63.0±2.4	62.3±3.6	59.9±4.4	<0.001	0.498	<0.001	<0.001
Sector 6 (N)	63.1±1.9	61.1±2.7	60.4±3.6	<0.001	0.075	<0.001	0.029
RNFLT (㎛) *							
Sector 1 (T)	80.3±13.6	74.7±13.1	57.0±15.4	<0.001	0.045	<0.001	<0.001
Sector 2 (IT)	141.2±30.0	110.4±39.5	55.7±34.1	<0.001	<0.001	<0.001	<0.001
Sector 3 (ST)	131.9±27.4	116.5±26.2	73.4±34.0	<0.001	0.025	<0.001	<0.001
Sector 4 (IN)	116.8±30.4	105.6±28.9	66.0±25.1	<0.001	0.042	<0.001	<0.001
Sector 5 (SN)	111.1±26.8	98.8±20.6	76.2±26.6	<0.001	0.039	<0.001	<0.001
Sector 6 (N)	76.9±14.9	73.5±14.4	60.2±20.1	<0.001	0.512	<0.001	0.001

Results of the numerical variables are presented as a unique value or as the mean±standard deviation.D=diopters, CCT=central corneal thickness, dB=decibel, MD=mean deviation, PSD=pattern standard deviation, pVD=peripapillary vessel density, RNFLT=retinal nerve fiber layer thickness, T=temporal, IT=inferotemporal, ST=superotemporal, IN=inferonasal, SN=superonasal, N=nasal.*Statistical significance was tested with the one-way analysis of variance test.†Statistical significance was tested with the Chi-square test.‡Intergroup ANOVA testing was performed using the mean values. If *P* values were less than 0.05, post hoc analysis (Turkey's test) was performed; §*P*-value for the post hoc analysis of the normal subjects and mild stage in the glaucoma group; ‖*P*-value for the post hoc analysis of the normal subjects and moderate-to-severe stage in the glaucoma group; ¶*P*-value for the post hoc analysis of the mild and moderate-to-severe stage in the glaucoma group

Sakaguchi *et al*. has reported that the relationship between sectoral VD and functional VF is stronger than the RNFL-VFS relationship across all sectors, proposing that the VD showed a more uniform correlation with VFS than RNFLT and may be more advantageous than RNFLT in terms of its structure-function relationship in glaucoma.[16] Akil *et al*. showed that the pVD using OCT-A could differentiate early glaucoma from pre-perimetric glaucoma and normal eyes.[17] In early glaucoma, the present study showed that pVD and VFS were significantly correlated in all sectors, while pRNFLT and VFS were only significantly correlated in ST and IT sectors. Therefore, our findings suggest that vascular density is a more sensitive parameter than RNFLT for detecting functional damage in early glaucoma. Consistent with previous studies,[18,19] our study shows that the average VD is an independent determinant of VF MD in glaucoma. Lee *et al*.[18] showed that decreased VD was significantly associated with the severity of glaucomatous functional damage after adjusting for structural parameters, such as pRNFLT, rim area, and disc area. Global and sectoral VDs are thus meaningful measurements for evaluating the relationship between structure and function in glaucoma.

The present study revealed that glaucomatous papillomacular defects are significantly associated with corresponding VD as well as RNFLT. This finding differs from peripheral field defects which are strongly associated with only RNFLT. Penteado *et al*. observed that macular VD was significantly associated with central VFS in a multivariate analysis.[20] Holló G *et al*. also found that temporal pVD significantly correlated with the corresponding VFS in glaucomatous eyes, suggesting that glaucoma-related vascular dysfunction in the particularly stable papillomacular area may start at an early stage. However, the previous studies lack a multivariate analysis to determine the factors associated with VFS.[21]

In our study, the pRNFLT and pVD in the IT sectors show the best diagnostic performance for detecting glaucoma. This finding is consistent with previous studies showing the greatest AUROC in IT or ST sectors, which are more vulnerable to glaucomatous damage than other sectors.[6,7]

The pVD-VFS relationship in the central field is independently and significantly correlated in our study, suggesting that VD in glaucomatous eyes with central defects must be considered as a significant factor affecting VF defects. In the previous

Table 2: Sectoral multivariate linear regression analysis of independent parameters on the VFS in normal and total glaucoma group.

Normal subject	Sector 1 (T)		Sector 2 (IT)		Sector 3 (ST)		Sector 4 (IN)		Sector 5 (SN)		Sector 6 (N)		Average	
	β^{+} *P*	$\beta^{\#}$ *P*	β^{+} *P*	$\beta^{\#}$ *P*	β^{+} *P*	$\beta^{\#}$ *P*	β^{+} *P*	$\beta^{\#}$ *P*	β^{+} *P*	$\beta^{\#}$ *P*	β^{+} *P*	$\beta^{\#}$ *P*	β^{+} *P*	$\beta^{\#}$ *P*
Age	-8.106 <0.001	-7.416 <0.001	-20.668 <0.001	-19.016 <0.001	-19.018 <0.001	-21.075 <0.001	-18.262 <0.001	-22.952 <0.001	-15.277 <0.001	-17.036 <0.001	-14.566 <0.001	-11.278 0.018	-15.983 <0.001	-17.174 <0.001
Gender (male)	22.796 0.640	54.260 0.249	78.822 0.461	90.346 0.316	120.588 0.405	273.310 0.081	48.594 0.738	84.292 0.583	68.734 0.494	166.279 0.082	36.362 0.740	76.629 0.512	98.490 0.853	128.510 0.128
SPH	-17.864 0.032	-8.268 0.507	-14.807 0.011	-8.171 0.722	16.585 0.087	17.447 0.656	40.673 0.213	28.623 0.486	42.829 0.111	16.415 0.506	-52.745 0.384	-11.306 0.723	34.251 0.185	5.939 0.786
CCT	0.129 0.876	0.108 0.875	0.172 0.926	-0.073 0.956	-0.034 0.989	0.954 0.667	-0.033 0.989	0.952 0.678	-1.262 0.460	-0.655 0.644	-2.406 0.194	-2.479 0.165	-0.572 0.711	-0.141 0.908
pRNFL	1.198 0.515	2.437 0.136	4.707 0.008	3.898 0.006	5.147 0.038	5.118 0.047	3.681 0.123	3.837 0.138	2.611 0.164	2.629 0.157	-4.387 0.233	-2.834 0.496	2.565 0.302	3.416 0.153
pVD	-10.073 0.553	-7.847 0.588	-6.262 0.861	-51.661 0.055	20.796 0.310	8.694 0.827	35.550 0.269	12.419 0.678	48.400 0.038	17.732 0.355	39.357 0.175	25.957 0.428	60.494 0.129	-13.769 0.718
HTN	-65.687 0.242	-57.866 0.236	-15.815 0.273	-19.937 0.819	-257.209 0.123	-141.456 0.363	-127.981 0.449	-65.253 0.671	-119.422 0.097	-139.019 0.149	-95.852 0.232	-79.479 0.491	-99.508 0.126	-87.067 0.294
DM	-112.793 0.084	-67.800 0.265	-212.705 0.141	-64.252 0.555	48.937 0.804	76.170 0.681	77.862 0.694	196.089 0.296	16.428 0.905	67.724 0.570	-91.960 0.256	-31.464 0.825	80.011 0.515	38.705 0.707
R^2		0.653		0.756		0.564		0.552		0.652		0.530		0.682
Total glaucoma	β^{+} *P*	$\beta^{\#}$ *P*	β^{+} *P*	$\beta^{\#}$ *P*	β^{+} *P*	$\beta^{\#}$ *P*	β^{+} *P*	$\beta^{\#}$ *P*	β^{+} *P*	$\beta^{\#}$ *P*	β^{+} *P*	$\beta^{\#}$ *P*	β^{+} *P*	$\beta^{\#}$ *P*
Age	-5.909 0.013	-5.955 0.015	-13.191 <0.001	-12.646 <0.001	-10.699 0.005	-16.747 <0.001	-11.959 <0.001	-11.830 <0.001	-9.557 0.011	-11.283 0.012	-13.232 0.002	-12.587 0.010	-10.739 0.001	-9.102 0.004
Gender (male)	38.115 0.557	16.198 0.765	31.721 0.790	47.322 0.556	137.495 0.353	75.380 0.501	13.331 0.875	10.195 0.883	38.09 0.706	15.256 0.871	-18.941 0.872	-1.913 0.986	22.691 0.801	26.405 0.685
SPH	10.459 0.919	13.117 0.340	9.232 0.724	33.707 0.103	20.967 0.520	29.676 0.294	12.469 0.501	18.748 0.293	13.318 0.556	50.710 0.138	10.140 0.996	37.798 0.184	5.441 0.784	22.069 0.188
CCT	2.016 0.031	0.684 0.373	0.748 0.666	0.374 0.747	3.188 0.149	1.484 0.353	-0.142 0.909	-0.129 0.897	2.013 0.180	1.503 0.264	3.698 0.028	2.788 0.073	1.909 0.146	1.140 0.222
pRNFL	9.714 <0.001	7.634 <0.001	8.864 <0.001	6.882 <0.001	12.304 <0.001	10.214 <0.001	5.959 <0.001	4.239 <0.001	8.378 <0.001	4.864 <<0.044	11.189 <0.001	4.745 <<0.038	11.031 <0.001	6.336 <<0.003
pVD	50.131 <0.001	26.082 <0.007	62.835 <0.002	14.738 <0.198	99.609 <0.001	31.050 <0.108	43.831 <0.001	20.056 <0.104	52.443 <0.001	23.263 <0.132	74.413 <0.001	46.299 <0.238	97.542 <0.001	49.461 <0.010
HTN	0.5645 0.994	-2.173 0.968	20.935 0.869	-34.453 0.678	-107.051 0.502	-122.049 0.294	-97.294 0.282	-106.099 0.140	-92.052 0.404	-141.176 0.159	-97.732 0.275	-202.248 0.076	-68.772 0.477	-105.250 0.121
DM	-7.215 0.993	-68.277 0.307	21.547 0.887	-87.943 0.396	15.004 0.937	22.946 0.869	-50.729 0.638	-61.356 0.494	-92.376 0.481	-133.906 0.261	-11.041 0.941	-70.190 0.612	-19.719 0.864	-98.731 0.235
R^2		0.721		0.808		0.764		0.706		0.614		0.601		0.785

Statistical significant values are in bold type.Backward multiple linear regression method applied. Model assumption is fulfilled.β^{+} Crude regression coefficient by single linear regression. $\beta^{\#}$ Adjusted regression coefficient by multiple linear regression.SPH=spherical equivalent, CCT=central corneal thickness, pRNFL=peripapillary retinal nerve fiber layer thickness, pVD=peripapillary vessel density, HTN=hypertension, DM=diabetes mellitus, T=temporal, IT=inferotemporal, ST=superotemporal, IN=inferonasal, SN=superonasal, N=nasal

Table 3: Comparison of the regional diagnostic abilities for detecting different stages of glaucoma between peripapillary vascular density (pVD) and retinal nerve fiber layer thickness (pRNFLT)

Stage	Sector	pVD	pRNFLT	*P**
Total				
	Sector 1 (T)	0.746 (0.669-0.823)	0.744 (0.666-0.821)	0.959
	Sector 2 (IT)	0.843 (0.781-0.904)	0.833 (0.769-0.897)	0.759
	Sector 3 (ST)	0.725 (0.644-0.805)	0.781 (0.709-0.853)	0.214
	Sector 4 (IN)	0.709 (0.627-0.791)	0.747 (0.671-0.823)	0.402
	Sector 5 (SN)	0.678 (0.589-0.767)	0.730 (0.649-0.810)	0.284
	Sector 6 (N)	0.680 (0.595-0.764)	0.659 (0.573-0.745)	0.244
Mild				
	Sector 1 (T)	0.603 (0.489-0.717)	0.624 (0.517-0.730)	0.778
	Sector 2 (IT)	0.714 (0.614-0.814)	0.718 (0.615-0.821)	0.945
	Sector 3 (ST)	0.654 (0.547-0.761)	0.664 (0.561-0.767)	0.881
	Sector 4 (IN)	0.589 (0.475-0.703)	0.584 (0.474-0.694)	0.941
	Sector 5 (SN)	0.523 (0.406-0.640)	0.635 (0.531-0.739)	0.098
	Sector 6 (N)	0.621 (0.513-0.730)	0.559 (0.447-0.671)	0.303
Moderate-to-severe				
	Sector 1 (T)	0.889 (0.825-0.953)	0.863 (0.791-0.936)	0.544
	Sector 2 (IT)	0.972 (0.943-1.000)	0.948 (0.904-0.992)	0.163
	Sector 3 (ST)	0.845 (0.749-0.941)	0.898 (0.839-0.958)	0.381
	Sector 4 (IN)	0.828 (0.748-0.908)	0.910 (0.849-0.971)	0.073
	Sector 5 (SN)	0.733 (0.634-0.832)	0.824 (0.746-0.903)	0.071
	Sector 6 (N)	0.738 (0.643-0.834)	0.758 (0.662-0.855)	0.662

Variables are presented as the areas under the receiver operating characteristics curves (AUROC), with 95% confidence interval values provided in parentheses. T=temporal, IT=inferotemporal, ST=superotemporal, IN=inferonasal, SN=superonasal, N=nasal. *Comparison of the area under the receiver operating characteristics curves using DeLong *et al.*'s method

studies, glaucomatous eyes with central field defects tended to have vulnerable vasculature in the optic nerve. In addition, pVD has been better than pRNFLT at reflecting functional impairment in glaucoma in the central area. Therefore, the strong relationship between vasculature and function in the central field may be due to the ischemic pathogenic nature of the glaucomatous damage. Moreover, in the IT and ST sectors known as vulnerable sectors to glaucomatous damage,[22] RNFLT has had the greatest diagnostic ability as well as significant association with functional parameters. Measuring RNFLT in OCT is also essential for the diagnosis of glaucoma.

There are several limitations to the present study. First, this study included patients with primary open-angle glaucoma who also had normal-tension glaucoma (NTG) that is more vulnerable to vascular insufficiency. Thus, there is a possibility for overestimation of the vessel structure-function relationship. Second, we were not able to exclude the effects of anti-glaucoma eye drops or other systemic vasoactive medications that can alter retinal vessel diameter. The relationship between pVD and VFS revealed in this study should therefore be interpreted with caution. Third, peripapillary atrophy may have affected pVD in myopic eyes. However, we excluded high myopia above -6D, so the effect on pVD of peripapillary atrophy was minimized. Fourth, in the sectoral relationship between the structure (pVD and RNFL) and VF defect, we used the Garway-Heath map[15] to see which relationship is better. Therefore, the temporal sector could not be divided into upper-temporal and lower-temporal sectors along the histological horizontal raphe. Finally, this is a cross-sectional study and we cannot conclude that the observed pVD is the primary pathogenic mechanism in glaucoma and precedes IOP elevation or RNFL damage. Further longitudinal studies are required to tease out this distinction.

Conclusion

To the best of our knowledge, this is the first report to investigate the sectoral relationship between VD, RNFLT, and VFS in both glaucoma and normal subjects and compare their VFS with its associated factors to corresponding peripapillary regions based on the Garway-Heath map. Since the relationship between pVD-VFS in the papillomacular nerve fiber bundle region was significant, pVD using OCT-A in this area is the useful parameter to evaluate structure and function within the paracentral area in glaucoma.

Declaration of patient consent

The authors certify that they have obtained all appropriate patient consent forms. In the form the patient(s) has/have given his/her/their consent for his/her/their images and other clinical information to be reported in the journal. The patients understand that their names and initials will not be published and due efforts will be made to conceal their identity, but anonymity cannot be guaranteed.

Financial support and sponsorship

Nil.

Conflicts of interest

There are no conflicts of interest.

References

1. Burgoyne CF, Morrison JC. The anatomy and pathophysiology of the optic nerve head in glaucoma. J Glaucoma 2001;10:S16-8.
2. Kumar RS, Anegondi N, Chandapura RS, Sudhakaran S, Kadambi SV, Rao HL, *et al*. Discriminant function of optical coherence tomography angiography to determine disease severity in glaucoma. Investig Ophthalmol Vis Sci 2016;57:6079-88.
3. Zhang S, Wu C, Liu L, Jia Y, Zhang Y, Zhang Y, *et al*. Optical coherence tomography angiography of the peripapillary retina in primary angle-closure glaucoma. Am J Ophthalmol 2017;182:194-200.
4. Park JH, Yoo C, Park J, Kim YY. Visual field defects in young patients with open-angle glaucoma. J Glaucoma 2017;26:541-7.
5. De Moraes CG, Liebmann JM, Park SC, Tello C, Ritch R, Teng CCW. Initial parafoveal versus peripheral scotomas in glaucoma: Risk factors and visual field characteristics. Ophthalmology 2011;118:1782-9.
6. Chung JK, Hwang YH, Wi JM, Kim M, Jung JJ. Glaucoma diagnostic ability of the optical coherence tomography angiography vessel density parameters. Curr Eye Res 2017;42:1458-67.
7. Rao HL, Pradhan ZS, Weinreb RN, Reddy HB, Riyazuddin M, Dasari S, *et al*. Regional comparisons of optical coherence tomography angiography vessel density in primary open-angle glaucoma. Am J Ophthalmol 2016;171:75-83.
8. Akagi T, Iida Y, Nakanishi H, Terada N, Morooka S, Yamada H, *et al*. Microvascular density in glaucomatous eyes with hemifield visual field defects: An optical coherence tomography angiography study. Am J Ophthalmol 2016;168:237-49.
9. Chen CL, Zhang A, Bojikian KD, Wen JC, Zhang Q, Xin C, *et al*. Peripapillary retinal nerve fiber layer vascular microcirculation in glaucoma using optical coherence tomography–based microangiography. Investig Ophthalmol Vis Sci 2016;57:475-85.
10. Lee EJ, Lee KM, Lee SH, Kim TW. OCT angiography of the peripapillary retina in primary open-angle glaucoma. Investig Ophthalmol Vis Sci 2016;57:6265-70.
11. Liu L, Jia Y, Takusagawa HL, Pechauer AD, Edmunds B, Lombardi L, *et al*. Optical coherence tomography angiography of the peripapillary retina in glaucoma. JAMA Ophthalmol 2015;133:1045-52.
12. Danthurebandara VM, Sharpe GP, Hutchison DM, Denniss J, Nicolela MT, McKendrick AM, *et al*. Enhanced structure–function relationship in glaucoma with an anatomically and geometrically accurate neuroretinal rim measurement. Investig Ophthalmol Vis Sci 2014;56:98-105.
13. Nilforushan N, Nassiri N, Moghimi S, Law SK, Giaconi J, Coleman AL, *et al*. Structure-function relationships between spectral-domain OCT and standard achromatic perimetry. Investig Ophthalmol Vis Sci 2012;53:2740-8.
14. Chen CL, Bojikian KD, Wen JC, Zhang Q, Xin C, Mudumbai RC, *et al*. Peripapillary retinal nerve fiber layer vascular microcirculation in eyes with glaucoma and single-hemifield visual field loss. JAMA Ophthalmol 2017;135:461-8.
15. Garway-Heath DF, Poinoosawmy D, Fitzke FW, Hitchings RA. Mapping the visual field to the optic disc in normal tension glaucoma eyes. Ophthalmology 2000;107:1809-15.
16. Sakaguchi K, Higashide T, Udagawa S, Ohkubo S, Sugiyama K. Comparison of sectoral structure-function relationships in glaucoma: Vessel density versus thickness in the peripapillary retinal nerve fiber layer. Investig Ophthalmol Vis Sci 2017;58:5251-62.
17. Akil H, Huang AS, Francis BA, Sadda SR, Chopra V. Retinal vessel density from optical coherence tomography angiography to differentiate early glaucoma, pre-perimetric glaucoma and normal eyes. PLoS One 2017;12:e0170476. doi: 10.1371/journal.pone. 0170476.
18. Lee J, Kook MS, Choi J, Shin JW, Kwon J. Regional vascular density–visual field sensitivity relationship in glaucoma according to disease severity. Br J Ophthalmol 2017;101:1666-72.
19. Yarmohammadi A, Zangwill LM, Diniz-Filho A, Suh MH, Yousefi S, Saunders LJ, *et al*. Relationship between optical coherence tomography angiography vessel density and severity of visual field loss in glaucoma. Ophthalmology 2016;123:2498-508.
20. Penteado RC, Zangwill LM, Daga FB, Saunders LJ, Manalastas PIC, Shoji T, *et al*. Optical coherence tomography angiography macular vascular density measurements and the central 10-2 visual field in glaucoma. J Glaucoma 2018;27:481-9.
21. Holló G. Comparison of peripapillary oct angiography vessel density and retinal nerve fiber layer thickness measurements for their ability to detect progression in glaucoma. J Glaucoma 2018;27:302-5.
22. Quigley HA, Addicks EM. Regional differences in the structure of the lamina cribrosa and their relation to glaucomatous optic nerve damage. Arch Opthalmol 1981;99:137-43.